The Effect of Nanostructured MnOx Crystallographic Phase and Particle Size in the Catalytic Decomposition of Hydrogen Peroxide for Environmental Remediation of Effluents

*David Delgado Vigil, Francisco Paraguay Delgado, Virginia Collins-Martínez, Alejandro López-Ortiz**

Centro de Investigación en Materiales Avanzados S. C. Chihuahua, México.
**Author to whom correspondence should be addressed, email:*
alejandro.lopez@cimav.edu.mx

Introduction

In the recent years there has been an increased interest on research focused on nanocrystalline materials due to their singular nanostructure, physical, mechanical, optical, electronic and catalytic properties. The effect of particle size on these properties has allowed the development of novel materials with applications in micro devices such as MEMS and in catalytic micro reactors for small power generation in portable electronic devices [1, 2].

Manganese oxides are among these nanometric materials with a wide variety of applications. These oxides have been used in electrode manufacturing [3] and selective catalytic oxidation applications such as nitrogen and carbon oxides elimination in exhaust gases [4], as well as in the preparation of magnetic materials [5].

The nanometric nature of these oxides produces a particle size effect that is reflected in an increase in their specific surface area generating outstanding catalytic properties compared with common industrial catalytic materials which present particle sizes in the order of microns.

Among the many expected advantages that nanometric catalysts produce is the effect that mass transport and kinetic limitations can be significantly reduced due to greater interactions of these particles with the reactive medium. For example, a greater surface area to volume ratio has significantly increased the oxygen adsorption in the NO_x and CO catalytic oxidation [5].

Past investigations have focused on the effect of temperature on the preparation of thermally metastable nanoparticle mixtures of manganese oxides in catalytic applications. Chen et al. [6] synthesized Mn_2O_3 by chemical oxidation of Mn^{+2} using H_2O_2 in a alkaline medium. Manthiram et al. [7, 8] studied the reduction of $KMnO_4$ with KBH_4 in aqueous solution to obtain mixtures of binary and ternary manganese oxides. Manganese oxides have been also prepared by other techniques such as hydrothermal [9-11], spray pyrolysis [12], sol gel [13] and mechanical alloy milling [14].

Nevertheless, these synthesis techniques often produce amorphous nanoparticles, and in order to produce crystalline materials, a thermal treatment at relatively high temperatures is needed consequently increasing the average particle size of these oxides. This udesired particle growth generates a significant surface area reduction that ultimately is traduced in loss of catalytic activity. An important disadvantage of the ball milling technique, resides in the fact that during the synthesis process certain impurities are often introduced to the catalytic material thus, contaminating the catalyst with impurities that may harm its catalytic performance.

In recent studies several researchers have introduced certain modifications to the previous precipitation techniques employed for the synthesis of different metal oxide nanoparticles [15-18]. In these syntheses, the precursors and kind of precipitant were varied in order to decrease the synthesis temperature. However, there are no reports of studies that explicitly are focused towards the synthesis of manganese oxides through chemical precipitation at low temperatures ($T \leq 300°C$).

Manganese oxides are well known by their catalytic properties in different selective oxidation processes such as hydrogen peroxide decomposition [19-21]. Therefore, in the present study this process was selected as a reaction model to study the particle size effect on this reaction system.

Therefore, the objective of the present research was aimed on the study of the type of precipitant effect on the particle size and crystalline phase towards the synthesis of nanosized manganese oxides. Additionally, the evaluation of the catalytic activity of the nanosized manganese oxides during the decomposition of hydrogen peroxide will be used to reveal which feature (particle size or crystalline phase) presents the greater influence on the catalytic activity.

Experimental

Synthesis

Manganese oxide nanoparticles were prepared through chemical precipitation employing two different precipitants and compared against reagent grade manganese oxide. The first synthesis consisted in a adaptation of the synthesis used for preparation of nanostructured Au/MnO_2 catalysts by Luengnaruemitchaia [15]. 250 ml of a 0.3M solution of $Mn(NO_3)_2$ (Merck) were slowly added, through a peristaltic pump (5 ml/min, 55°C, pH = 9.5) to 500 ml of a 0.2M solution of Na_2CO_3 (Merck) to precipitate $MnCO_3$. The precipitate was washed several times with deionized water, dried at 100°C overnight and calcined at 300°C for five hours in a box-heated air furnace. The resulting sample was named Mn-1. The second synthesis was based on an adaptation of the procedure reported by Xiang et al. [22] for the synthesis of NiO nanoparticles. 250 ml of a 0.3M solution of $Mn(NO_3)_2$ (Merck) were slowly added, through a peristaltic pump (5 ml/min, 55°C, pH = 9.5) to 500 ml of a 0.2M solution of NH_4OH (J. T. Baker) to precipitate $Mn(OH)_2$. The precipitate was washed several times with deionized water, dried at 100°C overnight and calcined at 300°C for five hours in a box-heated air furnace. The obtained sample was named Mn-2. Finally, MnO_2 (Merck reagent grade) was used for comparison purposes and named β-MnO_2.

Characterization

BET surface area determination of the samples was performed in an Autosorb-1 Gas Sorption System (Quantachrome Co.). X-Ray diffraction (XRD) crystal structure was determined by a Phillips X-Pert MPD diffractometer using monochromatized CuKα radiation. Morphology and particle size of the nanostructured catalysts were studied by transmission electron microscopy (TEM) in a Phillips CM200. The morphology of the commercial MnO_2 was studied in a scanning electron microscopy (SEM) JEOL JSM-5800LV.

Catalytic Activity

Catalytic activity of the synthesized materials was evaluated by measuring the oxygen evolution (gasometry) as a product of the catalytic decomposition of H_2O_2 through the following reaction:

$$H_2O_2\,(l) = H_2O\,(l) + O_2\,(g) \qquad (1)$$

The procedure reported by Deraz [23] was modified for a careful monitoring of the oxygen evolution which consisted in: 10 mg of catalyst was added to an Erlenmeyer flask containing distilled water and sonicated for 30 minutes. Afterwards, the flask was equipped with a thermometer, septa and a plastic micro-tubing and finally, hermetically sealed. The micro-tubing was connected to a sealed-inverted volumetric burette used to measure the water displacement by gas evolution. During reaction, the flask was kept at constant stirring and 25°C. At zero time the required amount of H_2O_2 (35% Fagalab) was injected through the septa to obtain a solution of 0.5%V H_2O_2 within the flask. Finally, the generated volume of oxygen was measured using the burette at several time intervals until reaction completion. Collected data were analyzed to evaluate the catalytic activity (rate constant, k) for each material.

Results and Discussion

XRD refraction patterns of Mn-1, Mn-2 and β-MnO_2 are shown in Figure 1. Mn-1 catalyst presents a mixture of three crystalline phases of manganese oxides: δ-MnO_2 (Birnessite), Mn_5O_8 and Mn_3O_4 (Hausmannite). This mixture of manganese oxide phases was also reported by Luengnaruemitchaia et al. [15]. Sample Mn-2 XRD pattern presents only the Mn_5O_8 phase, while the XRD pattern of commercial MnO_2 (reference material) shows only the β-MnO_2 phase (Pyrolusite).

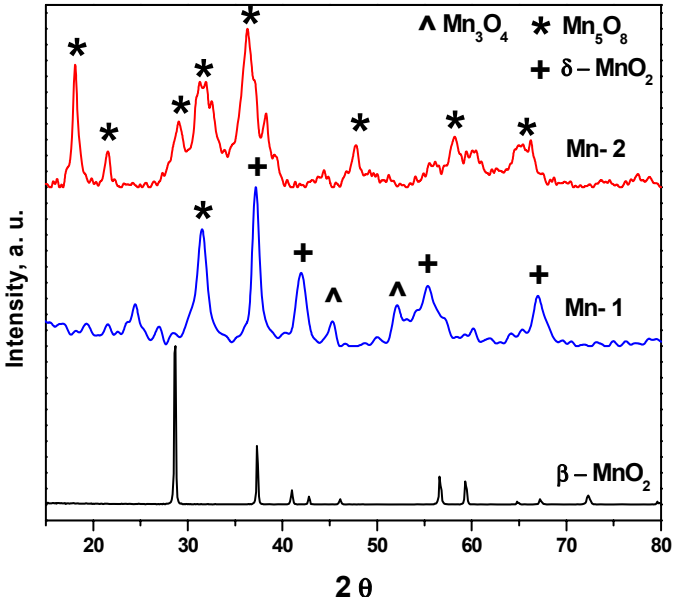

Figure 1. XRD results of synthesized Mn-based catalysts

Figure 2 presents TEM images of Mn-1 and Mn-2 catalysts.

In this Figure it is observed that Mn-1 catalyst is composed by irregular-shape nanoparticles with sizes in the range of 5-10 nm, whereas for the Mn-2 catalyst spherical-shape nanoparticles are observed with an average size of about 20 nm.

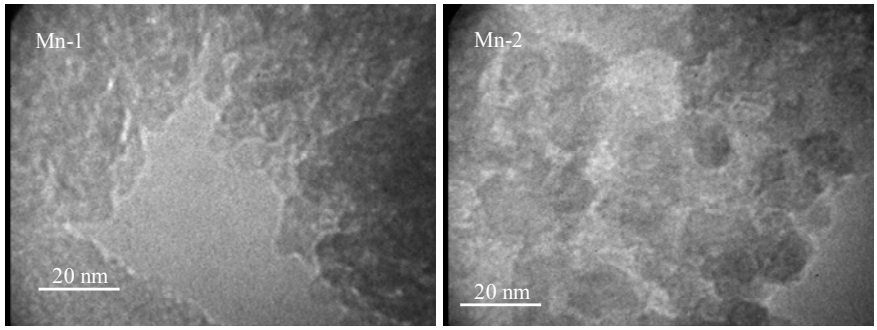

Figure 2. TEM images of catalysts Mn-1 and Mn-2

Figure 3 shows a SEM image of the β-MnO_2 catalyst. In this Figure it can be observed a morphology of irregular plate-like crystals with average particle sizes in the range of 50-100 μm.

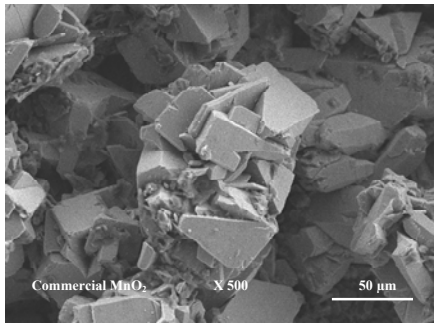

Figure 3. SEM image of commercial MnO_2 catalyst

Table 1 presents BET surface area results of studied catalysts in the present research. Surface areas of the Mn-1 and Mn-2 catalysts were 98 and 59 m^2/g, respectively. Apparently, sodium carbonate, the precipitant agent of catalyst Mn-1 generated smaller nanoparticles (dp ~ 5-10 nm) than catalyst Mn-2, which consequently was reflected in a greater surface area. While, the use of ammonium hydroxide as precipitant in catalyst Mn-2 produced particles of about 20 nm that were traduced in a relatively smaller surface area than catalyst Mn-1. This effect can be related to the inherent precipitation process originated by each of the precursors. When Na_2CO_3 is used as precipitant, the precipitate (manganese carbonate, Mn-1) is formed at a relatively constant pH. While an inherently and uneven change of pH during the precipitation process occurs when ammonium hydroxide is used as precipitant in Mn-2 catalyst [24]. The use of ammonium hydroxide solution in the present research resulted in the formation of manganese oxide particles greater than 10 nm. These results agree with results reported by Torres Sanchez et al. [24].

Table 1. BET Surface area and rate constants of catalytic H_2O_2 decomposition reaction

Catalyst	S (BET), m^2 g^{-1}	k, min^{-1} g^{-1}	k_{int}, min^{-1} m^{-2}
Mn-1	98	230	2.3
Mn-2	59	302	5.2
β-MnO_2	8	0.1	0.01

Also in Table 1 catalytic activity results are reported for the decomposition of hydrogen peroxide. Obtained results show that reaction (1) follows a first order kinetics in all cases. These results were corrected with respect to the non-catalytic H_2O_2 auto-decomposition reaction, which was previously determined to be about 1 cm_3 of O_2 released after 60 minutes of exposure to ambient temperature and normal light. The specific rate constant (k, $min^{-1}g^{-1}$) of the Mn-2 catalyst was approximately 1.3 times greater than Mn-1 and 3000 times greater than the one for commercial MnO_2. However, due to the fact that there are significant differences among surface areas of these catalysts it is suitable andf fair to compare their catalytic activity as a function of surface area through the use of the intrinsic rate constant (k_{int}, $min^{-1}m^{-2}$).

Once this calculation was performed (see Table 1) it is evident that the catalyst that presented the greatest activity of all was Mn-2. However, the proportionality in which these catalysts are now being compared has changed. For example, Mn-2 is twice as much active than Mn-1 catalyst and 520 times more active than commercial MnO_2.

Once surface area and catalyst amount effects have been accounted the other remaining effect that directly influence the catalytic activity of the studied reaction is the crystal structure of manganese oxide present in each catalyst presents.

According to Hasan et al. [25] the MnO_2 phase during the H_2O_2 decomposition suffers the loss of one of their oxygen atoms, which is traduced in the formation of the Mn_2O_3 crystal phase. Such a change in crystalline structure has been recently associated with a significant decrease in catalytic activity towards hydrogen peroxide decomposition. In contrast, the phases that are present in a mixture of valences as in Mn_5O_8 (= $Mn_2^{II}Mn_3^{IV}O_8$) and Mn_3O_4 (= $Mn^{II}Mn_2^{III}O_4$) have been demonstrated to produce similar catalytic activity as MnO_2 during the H_2O_2 decomposition reaction. This can be attributed to manganese atoms of different oxidation states coexisting within the same crystal network that apparently present an electron exchange interaction of the outside d-d layers. Therefore, this phenomenon is though to provide the needed environment of electronic mobility for the superficial redox activity [25]. Consequently, it is expected that Mn-2 catalyst that presents Mn_5O_8 as its predominant crystal phase, (a mixture of manganese valences) to be the one that produce the highest activity with respect to the other two catalysts (Mn-1 and MnO_2) that only showed one manganese oxidation state (MnO_2).

Furthermore, when comparing the intrinsic activity between Mn-1 and β-MnO_2 catalysts it is evident that the activity of Mn-1 (k_{int} = 2.3 $min^{-1}m^{-2}$) remains to be greater than the one observed for the β-MnO_2 catalyst (k_{int} = 0.01 $min^{-1}m^{-2}$). This can be attributed to the fact that Mn-1 catalyst presents, additionally to the Mn_2O_3 phase, the Mn_3O_4 phase. This crystal phase (Mn_3O_4) also provides the needed electron exchange within the outer d-d electronic layers responsible for the Mn-1 catalytic activity.

Conclusions

Precipitant agent sodium carbonate in Mn-1 catalyst produced particles with an average size in the range of 5-10 nm, which can be attributed to the relatively constant pH (pH = 8) that was achieved throughout the precipitation process. Meanwhile, the use of ammonium hydroxide as precipitant in the Mn-2 catalyst generated larger particles

with an average size of 20 nm. This resulted particle size was attributed to unavoidable pH variations that occurred during the precipitation process. Catalyst Mn-2 is the one that presented the highest activity towards H_2O_2 decomposition reaction among catalysts studied. The superior catalytic activity of Mn-2 was evident when both, the specific (per unit mass) and the intrinsic rate (per unit area) constants, were greater than the ones presented for other studied catalysts (Mn-1 and β-MnO_2). Specifically, the activity in terms of the intrinsic rate constant for catalyst Mn-1 (k_{int} = 2.3 $min^{-1}m^{-2}$) was about twice for Mn-1 catalyst and about 520 times the activity of catalyst β-MnO_2. Presumably, the main factor responsible for the superior activity of Mn-2 is though to be the Mn_5O_8 crystal phase present in this catalyst. Finally, Mn_5O_8 and Mn_3O_4 crystal phases, which present manganese atoms in different oxidation states within their crystal network, are though to promote the electronic mobility environment, presumably responsible for the greater surface redox activity.

Acknowledgments

The authors greatly appreciate the help of M. Sc. Enrique Torres, Eng. Wilber Antunez, Eng. Luis de la Torre Saenz and M. Sc. Oscar Ayala for their assistance during this work.

References

[1] P. G. Lacroix, R. Clement, K. Nakatani, J. Zyss, I. Ledoux, Sci. 263 (1994) 658.
[2] G. Schmid, Chem. Rev. 92 (1992) 1709.
[3] J. C. Z. Nardi, J. Electrochem. Soc. 132 (1985) 1787.
[4] L. Hegedeus, J. W. Beckman, W. H. Pan, J. P. Solor, eur. Appl. 345 (1989) 695.
[5] W. S. Seo, H. H. Jo, K. Lee, B. Kim, S. J. Oh, J. T. Park, Angew. Chem. Int. Ed. 43 (2004) 1115.
[6] Z. Chen, S. Tan, F. Li, J. Wang, S. Jin, Y. Zhang, J. Cryst. Growth Des. 180 (1997) 280.
[7] C. Tsang, J. Kim, A. Manthiram, J. Solid State Chem. 137 (1998) 28.
[8] S. Ching, J. A. Landdriggan, M. L. Jorgensen, N. Duan, S. L. Suib, C. L. O'Young, Chem. Mater. 7 (1995) 1064.
[9] C.H. Shomate, J. Amer. Chem. Soc. 65 (1943) 786.
[10] J.C. Southard, G.E. Moo, J. Amer. Chem. Soc. 64 (1942) 1769.
[11] I. Ursu, R. Alexandrescu, I.N. Mihailescu, J. Phys.Chem. B 19 (1986) 825.
[12] S. H. Ju, D. Y. Kim, H. Y. Koo, S. K. Hong, E. B. Jo, Y. C. Kang, J. Alloys Compd., Article in Press (2006).
[13] M. Kumar, U. Chandra, G. Parthasarathy, Mater. Lett., Article in Press (2006).
[14] S. H. Lee, Kyoung I. Moon, K. S. Lee, Intermetallics 14 (2006) 1.
[15] A. Luengnaruemitchai, D. T. K. Thoa, S. Osuwan, E. Gulari, Int. J. Hydrogen Energy 30 (2005) 981.
[16] H. Wang, J. Wang, W-D. Xiao, W-K. Yuan, Powder Technol. 111 (2000) 175.
[17] J. E. Sunstrom IV, W. R. Moser, and B. Marshik-Guerts, Chem. Mater., 8 (1996) 2061.
[18] D. G. Klissurski, E. L. Uzunova, Appl. Surf. Sci. 214 (2003) 370.
[19] K. Katz, Adv. Catal. 5 (1953) 177.
[20] J.S. Anderson, Annu. Rep. Chem. Soc. London., 43 (1946) 104.
[21] M.I. Zaki, M.A. Hasan, L. Pasupulety, K. Kumari, New J. Chem. 22 (1998) 875.
[22] L. Xiang, X.Y. Deng, Y. Jin, Scripta Mater. 47 (2002) 219.
[23] N-A. M. Deraz, Mater. Lett. 57 (2002) 914.
[24] R. M. Torres Sanchez, A. Ueda, K. Tanaka, M. Haruta, J. Catal., 168 (1997) 125.
[25] M. A. Hasan, M. I. Zaki, L. Pasupulety and K. Kumari, Appl. Catal. A., 181 (1999) 171.